ARTICLE

Self-Assembly of Colloidal Quantum Dots on the Scaffold of Triblock Copolymer Micelles

Mingfeng Wang,† Meng Zhang, James Li, Sandeep Kumar, Gilbert C. Walker, Gregory D. Scholes,* and Mitchell A. Winnik*

Department of Chemistry, University of Toronto, 80 St. George Street, Toronto, M5S 3H6 Ontario Canada

ABSTRACT This paper describes the co-self-assembly of a polystyrene-poly(4-vinylpyridine)-poly(ethylene oxide) triblock copolymer with CdSe nanocrystals (quantum dots, QDs) and with a styrene compatible phenylenevinylene conjugated polymer (MEH-PPV) in mixtures of chloroform and 2-propanol. The polymer itself (PS_{577}−$P4VP_{302}$−PEO_{852}, where the subscripts refer to the number average degree of polymerization) forms worm-like micelles when 2-propanol is added to a solution of the polymer in $CHCl_3$. In the presence of increasing amounts of QDs, the structures become shorter and form only spherical hybrid micelles (with QDs bound to the surface) at 4:1 QD/polymer w/w, accompanied by free QDs. These structures retain their colloidal stability in 2-PrOH, suggesting that even the free QDs bear a surface shell of block copolymer. The presence of MEH-PPV has no affect on this self assembly. One of the most remarkable observations occurred when the samples in 2-PrOH were centrifuged to remove the free QDs accompanying the hybrid micelles. The micelles sedimented, but upon redispersion in 2-PrOH, rearranged to form colloidally stable long branched cylindrical structures including cylindrical networks.

KEYWORDS: block copolymers • self-assembly • micelles • quantum dots • composites • colloidal nanocomposites

1. INTRODUCTION

Composites consisting of polymers and inorganic nanocrystals (NCs) are one of the most important advanced materials for a variety of applications (1−4). These nanocomposites not only combine the unique properties of each component but can also lead to new functions because of the interaction between the components. For example, nanocomposites of polymers and semiconductor nanocrystals (also called quantum dots (QDs)) show both mechanical flexibility inherent in the polymer and the unique size-dependent optoelectronic properties of the QDs. Moreover, the interaction between conjugated polymers and QDs can lead to photoinduced charge or energy transfer between these two components (5, 6). These new properties that derive from the conjugated-polymer/QD interaction in the nanocomposites have raised interest in their use in device applications, such as solar cells and light-emitting diodes (7, 8).

It is known that most high-quality colloidal NCs are synthesized through rapid injection of metal-organic precursors into a vigorously stirred flask containing a hot (normally 150−350 °C) coordinating solvent. The solvents usually used are mixtures of medium- or long-chain alkylphosphines R_3P, alkylphosphine oxides R_3PO (R = butyl or octyl), alkylamines, or acids (9−11). The advantages of this synthetic method include the high crystallinity and narrow size distribution of the NCs, as well as synthesis lattitude for size and shape control. Nevertheless, one of the inherent challenges for NCs synthesized by this approach is that the alkyl ligands on the surface of NCs are hydrophobic, electronically insulating, and not amenable to further functionalization.

For example, a common problem for blending polymers and the as-synthesized NCs described above is the uncontrolled aggregation of the NCs in the polymer matrix because of the poor interface compatibility, particularly when no specific interaction exists between the polymer and the NCs. For many applications of polymer/NC composites, the structure of the microphases formed through phase separation plays an essential role in determining the properties of the composites. To promote the interface compatibility between nanoparticles and polymers, several approaches such as "grafting to" (12−35), "grafting from" (36, 37), and in-situ formation of nanoparticles in polymer matrices (38−43) have been explored.

We have been interested in polymer−QD interactions for both homopolymers and copolymers bearing multiple pendant groups, such as tertiary amines, pyridines, and carboxylic acids, that show strong affinity to highly crystalline colloidal QDs, such as CdSe, core/shell CdSe/ZnS, and PbS (17−20, 22, 23, 25−27, 29−35). We use the term "highly crystalline" to emphasize that our interest has been focused on experiments involving QDs previously synthesized by high-temperature methods, as opposed to alternative approaches in which QDs were generated in situ at ordinary temperatures in the presence of block copolymers. Our initial experiments employed poly(*N*,*N*-dimethylaminomethyl acrylate) (PDMA), synthesized by free radical polymerization. We demonstrated that PDMA was able to displace alkyl ligands such as TOPO originally bound to the surface of CdSe QD particles, and these polymer molecules served as mulitidentate or multivalent ligands for the QD particles

* To whom correspondence should be addressed. E-mail: gscholes@chem.utoronto.ca (G.D.S.); mwinnik@chem.utoronto.ca (M.A.W.).
Received for review July 22, 2010 and accepted October 8, 2010
† Current address: Department of Chemistry and Biochemistry, Materials Research Laboratory, University of California, Santa Barbara.
DOI: 10.1021/am100645j

Published on Web 10/29/2010

(17, 22, 23, 25, 31, 32, 35). Such strong polymer/QD binding not only enhances the colloidal stability of individual QDs in a broad range of solvents but also promotes the dispersion of QD particles in polymer films (44). Moreover, one anticipates that advances in polymer chemistry and nanocrystal synthesis will provide additional opportunities to incorporate new functionalities into the thin and robust polymer shell of the polymer/QD adducts (6).

We recently took advantage of the multidentate polymer/QD interaction (17, 22, 23, 25, 31, 32) and the well-known self-assembly of block copolymers in solution (45, 46) to show that spherical "crew-cut" micelles of poly(styrene-*b*-4-vinylpyridine) (PS-*b*-P4VP) could serve as the structural motif for the spatially defined organization of colloidal QDs (such as CdSe, core/shell CdSe/ZnS or PbS) with conjugated polymers such as poly(3-hexylthiophene) (P3HT). The micelles formed when a solution of the components in chloroform was diluted with an alcohol such as 2-propanol (2-PrOH). At the same time, the nanocrystals became incorporated into the micelle corona consisting of P4VP chains that serve as the multidentate ligand, while the P3HT molecules were incorporated into the PS core of the micelles. An interesting feature of this experiment is that in the $CHCl_3$/2-PrOH mixed solvent and in a 2-PrOH solution obtained by evaporating the $CHCl_3$, all the QDs in the sample were incorporated into hybrid micelles. We did not observe any free QDs in transmission electron microscopy (TEM) images of these samples.

This concept of organizing highly crystalline nanocrystals via polymer self-assembly is also applicable to other morphologies of polymer self-assemblies such as PS-*b*-PAA vesicles (34). Nevertheless, this simple approach has its limitations. The hybrid QD/PS-*b*-P4VP spherical micelles tend to lose their colloidal stability, that is,they flocculated and precipitated from the selective solvent when the ratio of the QD/polymer was relatively high (29). Two possible factors contribute to this agglomeration include (i) bridging aggregation, in which some quantum dots become bound to the corona chains of adjacent micelles with an increasing ratio of QDs to micelles, and (ii) the collapse of P4VP brushes because of their binding to QDs thus providing less steric stabilization.

To overcome these problems, we designed an approach based on an ABC triblock copolymer in which the third block would serve to enhance the colloidal stability of the hybrid micelles by providing additional steric stabilization. We tested this idea using $PS_{577}-P4VP_{302}-PEO_{852}$ (where the subscripts refer to the number average degree of polymerization) as the triblock copolymer. The PS and P4VP blocks should serve the same role in the formation of micelle structures as described above, while the poly(ethylene oxide) (PEO) block should provide a stabilizing corona at the exterior of the structure. Samples prepared with CdSe/TOPO QDs in $CHCl_3$ as described above led to the formation of spherical hybrid micelles, but in addition, TEM images showed the presence of free QDs. To proceed with the experiments described below, we used centrifugation to separate the hybrid structures of interest from the free QDs. Surprisingly, redispersion of the QD/polymer sediment into 2-PrOH led to the formation of hybrid cylindrical micelles.

2. EXPERIMENTAL SECTION

2.1. Materials and Instruments. $PS_{577}-P4VP_{302}-PEO_{852}$ (M_n = 131 500, M_w/M_n = 1.2) was purchased from Polymer Source Inc. (Montreal, Canada) and used directly. This polymer is not soluble in THF, but soluble in $CHCl_3$. Poly(1-methoxy-4-(2-ethylhexyloxy)-p-phenylenevinylene) (MEH-PPV) (M_w = 80 000) was purchased from American Dye Source Inc. All of the QD samples were prepared by the traditional organometallic approach (9) at high temperature in the presence of trioctylphosphine oxide (TOPO) for both CdSe and CdSe/ZnS core/shell QDs. The QD samples were purified by precipitation in methanol to remove the excess ligands followed by redispersion in chloroform.

Optical absorption spectra were collected at room temperature on a Perkin-Elmer Lambda 25 spectrometer using 1.00 cm quartz cuvettes. The TEM images were taken using a Hitachi HD2000 STEM instrument. The samples for TEM measurements were prepared by placing a drop of a solution onto a carbon-coated copper grid (300 mesh). The excess solution on the grid was removed by touching the edge of the solution with a filter paper. After the samples were dried in air, TEM images were taken in the dark-field mode. Electron-dense objects appear bright in these images. All of the size analyses of TEM images were performed using Image J, a Java-based image processing program developed at the National Institutes of Health.

2.2. Preparation of $PS_{577}-P4VP_{302}-PEO_{852}$ Micelles: Effect of Solvent Ratios. $PS_{577}-P4VP_{302}-PEO_{852}$ (2.0 mg) was first dissolved in $CHCl_3$ (1.0 to 3.0 mL), a common good solvent for each block, followed by quick addition of 2-PrOH (8.0 mL). Then $CHCl_3$ (together with some 2-PrOH) was removed by attaching the vial, via an adaptor, directly to a rotary evaporator. The final volume of the mixture was adjusted to 8.0 mL with 2-PrOH, giving a final polymer concentration of 0.25 mg/mL.

2.3. $PS_{577}-P4VP_{302}-PEO_{852}$ Micelles: Effect of Polymer Concentration. Separate aliquots of $PS_{577}-P4VP_{302}-PEO_{852}$ (0.4, 1.0, 2.0, and 8.0 mL, 1.0 mg/mL in $CHCl_3$) were placed in 20 mL vials. $CHCl_3$ was removed with a rotary evaporator. Then 1.0 mL of $CHCl_3$ was added to each vial to redissolve the polymer. Finally, 8.0 mL of 2-PrOH was added to each solution. Then $CHCl_3$ (together with some 2-PrOH) was removed with a rotary evaporator. The final volume of the mixture was adjusted to 8.0 mL with 2-PrOH. Precipitation was observed in the sample with the highest polymer concentration (C_o = 8.0 mg/mL).

2.4. Preparation of $PS_{577}-P4VP_{302}-PEO_{852}$/CdSe(605) Hybrid Micelles. An aliquot of CdSe(605)/TOPO (8.0 mg/mL, in 0.5 mL of $CHCl_3$) was added to 1.0 mL of $PS_{577}-P4VP_{302}-PEO_{852}$ (2.0 mg/mL in $CHCl_3$) under stirring. Then 2-PrOH (4.0 mL) was added quickly to the mixture. The mixture was gently stirred to give homogeneous solution and stood for ~10 min under ambient conditions. Then $CHCl_3$ (together with some 2-PrOH) was removed with a rotary evaporator. The final volume of the mixture was adjusted to 8.0 mL with 2-PrOH.

2.5. $PS_{577}-P4VP_{302}-PEO_{852}$/CdSe(605) Hybrid Micelles: Effect of QD Concentrations. Measured amounts (0.2, 0.4, 0.8, and 1.6 mL) of CdSe(605)/TOPO solutions (3.4 mg/mL in $CHCl_3$) were added to 1.0 mL aliquots of $PS_{577}-P4VP_{302}-PEO_{852}$ (8 mg/mL in $CHCl_3$). These mixtures were mixed by gentle shaking. Then the $CHCl_3$ was removed by a rotary evaporator, and the dried residue was redispersed in 1.0 mL of $CHCl_3$. (Note: Both samples appeared turbid at a QD concentration of 1.4 and of 5.4 mg/mL but became clear upon ultrasonication (ultrasonic cleaning bath (Branson 1510, 60 W) for ~1 min). Then 8.0 mL of 2-PrOH was added to each sample. The mixture was gently stirred to give homogeneous solution and stood for ~10 min

under ambient conditions. After removal of $CHCl_3$ with a rotary evaporator, the volume of each sample was adjusted to 16 mL with 2-PrOH. As a control, a sample with the same concentration of the same polymer was prepared under the same condition. Each sample was diluted by 1/10 with 2-PrOH before the TEM measurements.

2.6. Separation of PS_{577}−$P4VP_{302}$−PEO_{852}/CdSe(605) Micelles by Centrifugation. An aliquot (in 2-PrOH) of CdSe(605)/PS_{577}−$P4VP_{302}$−PEO_{852} micelles prepared as described in section 2.4 was subjected to centrifugation at 14 000 rpm for 30 min. The supernatant was separated and the sediment was redispersed in 2-PrOH by a treatment in an ultrasonic cleaning bath (Branson 1510, 60 W) for ~20 s.

2.7. Preparation of PS_{577}−$P4VP_{302}$−PEO_{852}/MEH-PPV/CdSe(605) Hybrid Micelles. An aliquot of CdSe(605)/TOPO (5.4 mg/mL, in 0.5 mL of $CHCl_3$) was added to 1.0 mL of PS_{577}−$P4VP_{302}$−PEO_{852} (2.0 mg/mL in $CHCl_3$) under stirring, followed by addition of MEH-PPV (M_w = 80,000) (0.5 mL, 0.2 mg/mL in $CHCl_3$). The mixture was stirred continuously for ~10 min, after which the $CHCl_3$ was removed by a rotary evaporator. The dried residue was redispersed in 1.5 mL of $CHCl_3$. Then 2-PrOH (4.0 mL) was added to the mixture under stirring, after which the $CHCl_3$ (together with some 2-PrOH) was removed with a rotary evaporator. The final volume of the mixture was adjusted to 8.0 mL with 2-PrOH.

As a control, a sample of hybrid micelles of PS_{577}−$P4VP_{302}$−PEO_{852}/MEH−PPV without QDs was prepared by mixing a solution of PS_{577}−$P4VP_{302}$−PEO_{852} (1.0 mL, 2.0 mg/mL in $CHCl_3$), MEH−PPV (M_w = 80 000) (0.5 mL, 0.2 mg/mL in $CHCl_3$) and 0.5 mL of $CHCl_3$. The solvent was removed, and the sample was treated as described above.

2.8. Preparation of PS_{577}−$P4VP_{302}$−PEO_{852}/MEH−PPV/[CdSe/ZnS(485)] Hybrid Micelles. An aliquot of CdSe/ZnS(485)/TOPO (8.0 mg/mL, in 0.5 mL of $CHCl_3$) was added to 1.0 mL of PS_{577}−$P4VP_{302}$−PEO_{852} (1.0 mL, 2.0 mg/mL in $CHCl_3$) under stirring, followed by addition of MEH-PPV (M_w = 80 000) (0.5 mL, 0.2 mg/mL in $CHCl_3$). The mixture was stirred for ~10 min, after which the $CHCl_3$ was removed by a rotary evaporator. The dried residue was redispersed in 1.5 mL of $CHCl_3$, and then 2-PrOH (4 mL) was added to the mixture under stirring. Then $CHCl_3$ (together with some 2-PrOH) was removed with a rotary evaporator. The final volume of the mixture was adjusted to 8.0 mL with 2-PrOH.

Scheme 1. Self-Assembly of PS_{577}−$P4VP_{302}$−PEO_{852} with Colloidal CdSe/TOPO QDs in $CHCl_3$ /2-PrOH (3:8, v/v) Leads to the Formation of Polymer-Stabilized Individual QDs and Hybrid Spherical Micelles with QDs in the Mid-shell (P4VP) of the Micelles[a]

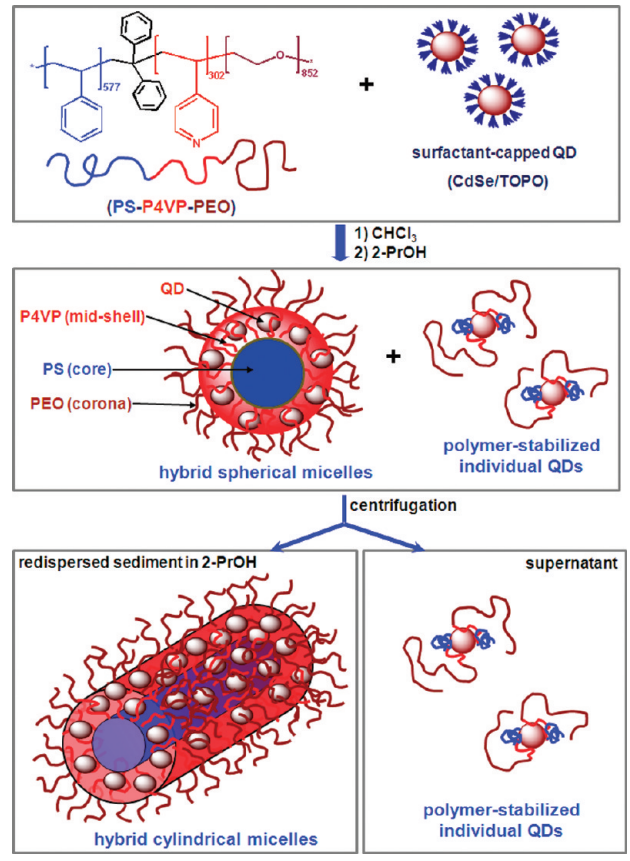

[a] Centrifugation of the mixture results in separation of the hybrid micelles that partitions to the sediment, while the individual QDs remain in the supernatant. The redispersion of the sediment into 2-PrOH results in hybrid cylindrical micelles.

3. RESULTS AND DISCUSSION

The amphiphilic triblock copolymer used here, PS_{577}−$P4VP_{302}$−PEO_{852} (M_n = 131 500, M_w/M_n = 1.2), is able to self-assemble into micellar structures in alcohol-rich selective solvents. For example, 2-PrOH is a poor solvent for PS but a good solvent for both P4VP and PEO. In this type of medium, we expect that PS_{577}−$P4VP_{302}$−PEO_{852} would form micelles with the collapsed PS block as the micellar core, surrounded by a P4VP shell and an exterior corona of PEO. We anticipated that when 2-PrOH was added to a $CHCl_3$ solution of this polymer plus CdSe QDs, in which the PS_{577}−$P4VP_{302}$−PEO_{852} micelles formed could capture the QD particles within the P4VP shell, with the pyridine groups serving as surface ligands for the QDs. The PEO chains on the exterior surface of the micelles should have no specific interaction with the QDs, but they should provide additional steric stabilization for the micelles (Scheme 1).

The protocol for self-assembly followed here was to dissolve the block copolymer plus any other components in chloroform, a common good solvent for all of the block copolymer components as well as the quantum dots and the conjugated polymer and then to add 2-propanol to promote assembly. In some experiments, we varied the amount of 2-PrOH that was added. In all instances, after a short period of time (~10 min), the solution was concentrated by rotary evaporation to remove $CHCl_3$ then diluted to a fixed volume with 2-PrOH. Thus all of the TEM images shown below were obtained from samples dissolved or dispersed in 2-PrOH that would contain at most traces of chloroform.

In the following sections, we first describe the self-assembly of PS_{577}−$P4VP_{302}$−PEO_{852} in a mixture of $CHCl_3$ and 2-PrOH. Then we describe the co-assembly of PS_{577}−$P4VP_{302}$−PEO_{852} in the presence of CdSe(605)/TOPO QDs in the same solvent mixture. We examine how the QD/polymer ratios affect the self-assembly of PS_{577}−$P4VP_{302}$−PEO_{852}. Finally, we present our strategy to separate the hybrid polymer/QD micelles from the polymer-stabilized QDs by centrifugation, followed by characterization of the sediment and the supernatant by TEM. We also show that we can incorporate the fluorescent conjugated polymer MEH-PPV into the core of these micelles.

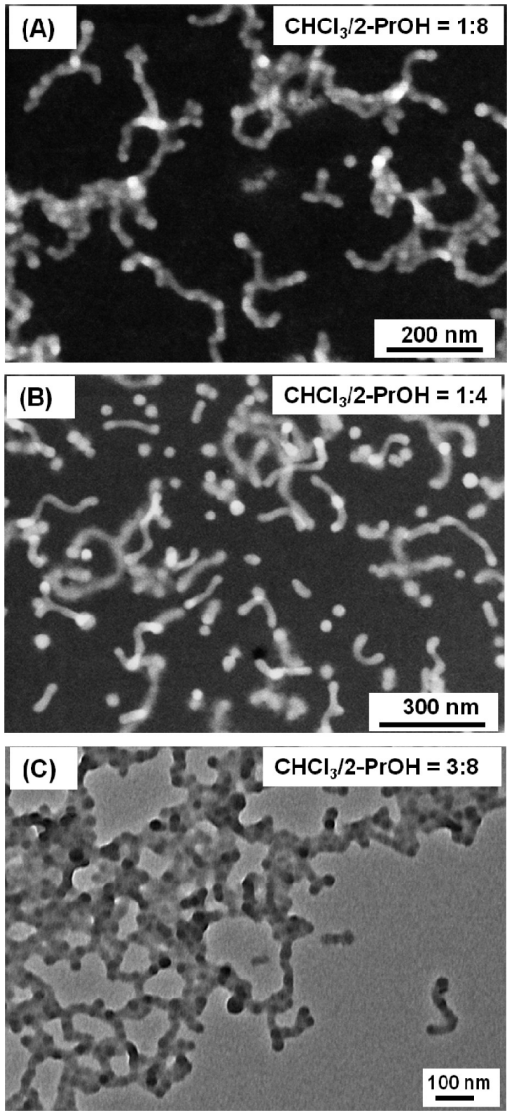

FIGURE 1. TEM (A, B, dark-field; C, bright field) images of the PS_{577}−$P4VP_{302}$−PEO_{852} micelles formed with different ratios of $CHCl_3$/2-PrOH: (A) 1:8, (B) 1:4, (C) 3:8 (v/v). After 10 min in that solution, the $CHCl_3$ was removed with a rotary evaporator, and the final concentration of the polymer was adjusted to 0.25 mg/mL with 2-PrOH.

3.1. Self-Assembly of PS_{577}−$P4VP_{302}$−PEO_{852} in $CHCl_3$/2-PrOH. The preparation of PS_{577}−$P4VP_{302}$-PEO_{852} micelles followed a similar procedure as we reported for the preparation of PS_{404}-$P4VP_{76}$ diblock copolymer micelles (29). The details of the sample preparation are described in the Experimental Section. Figure 1 shows TEM images of the PS_{577}−$P4VP_{302}$-PEO_{852} micelles formed in different ratios of $CHCl_3$/2-PrOH (varying from 1:8 to 3:8, v/v) after drying on a carbon-coated copper grid. A common feature of these TEM images is the coexistence of worm-like micelles with an average diameter of 24 ± 4 nm together with some spherical micelles (d = 34 ± 6 nm). Neither dilution of the micelles, for example, the ones formed in 1:4 (v/v) of $CHCl_3$/2-PrOH (Figure 1B), to 0.02 mg/mL with 2-PrOH nor a treatment of these diluted micelles in an ultrasonic bath (Branson 1510, 60 W) for 30 min led to any obvious change in the morphology or the population of the micelles (Figure S1, Supporting Information).

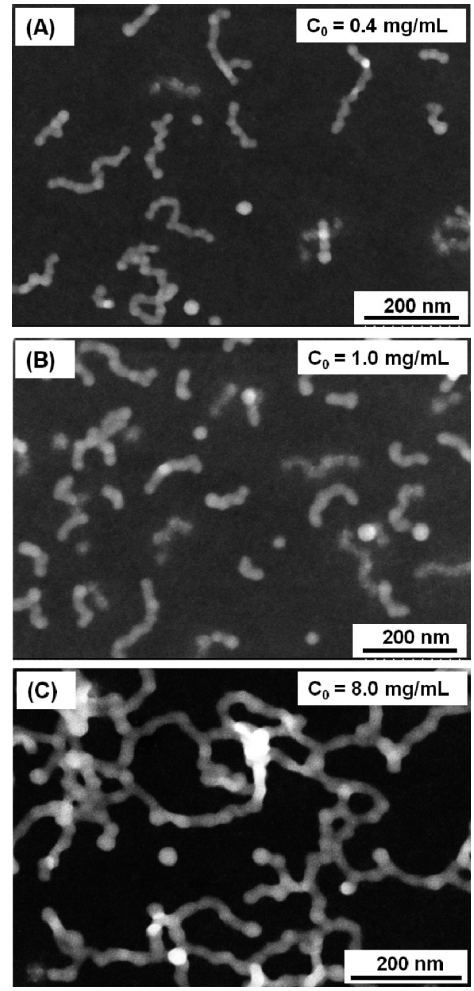

FIGURE 2. TEM (dark-field) images of the PS_{577}−$P4VP_{302}$−PEO_{852} micelles formed in $CHCl_3$/2-PrOH (1:8, v/v) at different initial concentrations in $CHCl_3$: (A) 0.4, (B) 1.0, and (C) 8.0 mg/mL. After removal of $CHCl_3$ with a rotary evaporator, the volume of each sample was adjusted to 8.0 mL with 2-PrOH. The sample shown in Figure C was diluted by 1/10 with 2-PrOH before the TEM grid was prepared.

Only small changes can be discerned in these TEM images. For example, there appear to be a larger fraction of spherical micelles in the sample prepared at a volume ratio of $CHCl_3$/2-PrOH of 1:4 (Figure 1B) compared to samples prepared in volume ratios of 1:8 (Figure 1A) and 3:8 (Figure 1C). Since these changes do not vary in a systematic way with solvent composition, and since the samples were all transferred after 10 min to 2-PrOH, we consider that these changes in solvent composition have relatively little influence on the block copolymer self assembly.

To examine whether polymer concentration (C_o) can affect the morphology of the PS_{577}−$P4VP_{302}$−PEO_{852} micelles, we prepared a series of polymer micelle samples keeping the solvent composition constant [$CHCl_3$/2-PrOH (1:8, v/v)]. The morphologies of these micelles examined by TEM are shown in Figure 2. At C_o = 0.4 mg/mL (Figure 2A), both worm-like and spherical micelles formed in $CHCl_3$/2-PrOH (1:8, v/v). There was no obvious change in the micellar

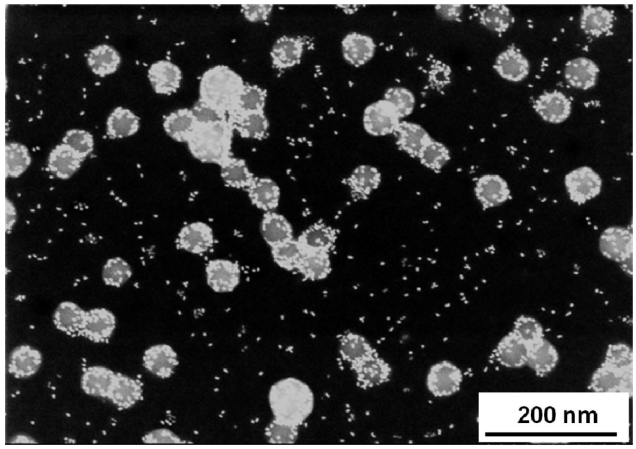

FIGURE 3. TEM (dark-field) image of the hybrid micelles formed by PS_{577}−$P4VP_{302}$−PEO_{852} and CdSe(605)/TOPO in $CHCl_3$/2-PrOH (3:8, v/v) at a final concentration of 0.25 mg/mL for the polymer and 1.0 mg/mL for the QDs, i.e. a QD/polymer ratio of 4:1 (by weight). The sample was transferred to 2-PrOH prior to preparing the TEM grid.

morphology when C_o was increased to 1.0 mg/mL (Figure 2B). At C_o = 2.0 mg/mL (Figure 1A), the average length of the worm-like micelles increased, while the number of coexisting spherical micelles appeared to be smaller. A dramatic change in the micellar morphology occurred when C_o was increased to 8.0 mg/mL (Figure 2C). In this case, a branched network of long cylindrical structures represented the major population of the colloidal species present, accompanied by a few spherical micelles. In this solution, we also noted the presence of white flocculated solids that settled to the bottom of the sample vial, possibly because of the formation of the large branched network structures similar to those reported by Zhang and Eisenberg (47).

The results above indicate that PS_{577}−$P4VP_{302}$−PEO_{852} in $CHCl_3$/2-PrOH (1:8, v/v) tends to form worm-like cylindrical micelles, accompanied by a small population of spherical micelles over a broad range of polymer concentrations.

3.2. Co-assembly of PS_{577}−$P4VP_{302}$−PEO_{852} and CdSe/TOPO QDs in $CHCl_3$/2-PrOH. The colloidal CdSe QDs that we used for the co-assembly with PS_{577}−$P4VP_{302}$−PEO_{852} were synthesized at high temperature in the presence of TOPO as the stabilizer (9). These spherical nanoparticles (denoted as CdSe(605)/TOPO) are monodisperse in size ($d = 5 \pm 1$ nm, measured by TEM) and show a band-edge absorption at 605 nm.

Figure 3 shows a dark-field TEM image of the co-assemblies of PS_{577}−$P4VP_{302}$−PEO_{852} and CdSe(605)/TOPO in $CHCl_3$/2-PrOH (3:8, v/v). One can discern spherical micelles decorated with many tiny bright spots. These correspond to the CdSe(605) QDs. These spherical micelles appear uniform in size (d = 45 ± 4 nm) and shape. Most of the micelles remain separate, although some aggregates can be seen. In previous experiments with CdSe QDs and PS-P4VP diblock copolymer (29), we were able to show that these aggregates did not exist in the micelle solution, but formed as the solvent evaporated on the TEM grid. In addition, one can see that there are some individual QD nanoparticles with no interaction with the micelles.

In an attempt to obtain further information about these micelles, we obtained atomic force microscopy (AFM) images for samples on a mica substrate. As shown in Figure S2 (Supporting Information), we observed discrete micelles without aggregates. In the phase image (Figure S2B, Supporting Information), the hybrid micelles appeared to have a pancake-like structure. A pancake morphology is consistent with the core/shell/shell structure of the micelles, wherein the rigid core of PS is surrounded by a mid-shell of P4VP and relatively soft corona of PEO. In the AFM images, it was very difficult to discern the individual QD particles that are observed easily by dark-field TEM, presumably because of their small size ($d \approx 5$ nm).

We were surprised to note the appearance of individual QDs not attached to polymer micelles, as seen in Figure 3. In a previous study (29) of CdSe/TOPO QDs with a PS-P4VP diblock copolymer (PS_{404}-*b*-$P4VP_{76}$) in similar mixtures of $CHCl_3$ and 2-PrOH, essentially all of the QD particles visible in the TEM images were incorporated into the corona of the PS-*b*-P4VP micelles. In the absence of the block copolymer, CdSe/TOPO QDs do not disperse in the $CHCl_3$/2-PrOH mixture employed in both sets of experiments. Thus finding free QDs in this solvent suggests that PS_{577}−$P4VP_{302}$−PEO_{852} binds to the QDs in $CHCl_3$, and the presence of the PEG chains is sufficient to stabilize some of the QDs outside of the micelles.

To test this idea, we carried out a control experiment to examine the binding of PS_{577}−$P4VP_{302}$−PEO_{852} to the QDs. In this experiment, excess *n*-hexane was added to a concentrated mixture of CdSe(605)/TOPO and PS_{577}−$P4VP_{302}$−PEO_{852} in $CHCl_3$. Essentially all of the QDs precipitated. The precipitate was separated by centrifugation (14 000 rpm, 10 min), leaving a nearly colorless supernatant. The sediment was purified by three cycles of redispersion of the sediment in ~1 mL of $CHCl_3$, followed by addition of 10 mL *n*-hexane. Then 8.0 mL of 2-PrOH was added to 1.0 mL of the QD/polymer dispersion in $CHCl_3$. Examination of this sample by TEM still showed the presence of some individual QD particles (Figure S3B, Supporting Information). Since CdSe/TOPO forms stable colloidal solutions in hexane, the formation of a colorless supernatant following the initial precipitation with hexane indicates that the pyridine groups of the polymer have replaced many of the TOPO groups on the QDs, rendering them insoluble in hexane. The observation of individual QDs following the successive sedimentation−redispersion cycles indicates that these particular QDs are effectively stabilized against incorporation into micelles by the polymer on their surface. A drawing of these types of polymer-stabilized individual QDs is depicted at the bottom right of Scheme 1.

3.3. Effect of QD/Polymer Ratio on the Co-assembly of CdSe(605)/PS_{577}−$P4VP_{302}$−PEO_{852} in $CHCl_3$/2-PrOH. The results described in section 3.1 indicate that PS_{577}−$P4VP_{302}$−PEO_{852} itself tends form worm-like cylindrical structures in $CHCl_3$/2-PrOH (from 1:8 to 3:8, v/v). Nevertheless, the co-assembly of PS_{577}−$P4VP_{302}$−PEO_{852} with CdSe(605)/TOPO led nearly exclusively to spherical hybrid

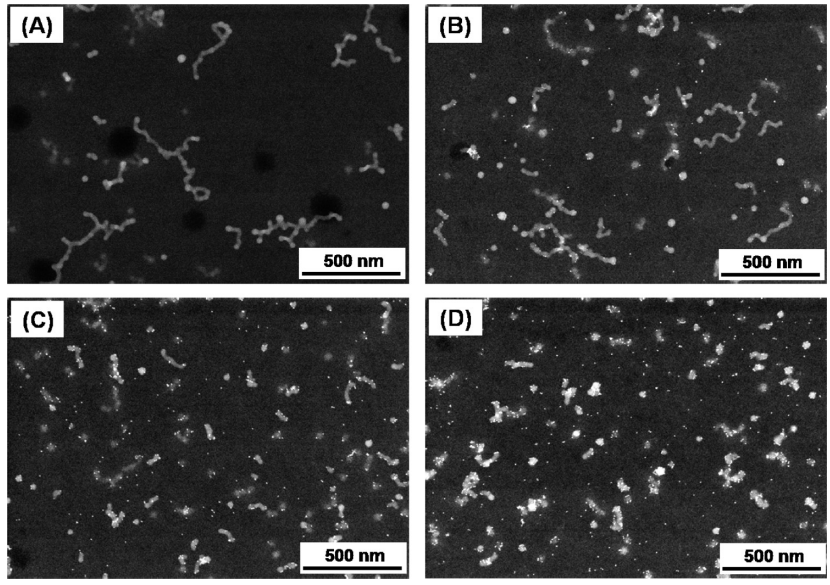

FIGURE 4. TEM (dark-field) images of the hybrid micelles formed by PS_{577}−$P4VP_{302}$−PEO_{852} and CdSe(605)/TOPO in $CHCl_3$ /2-PrOH (1:8, v/v) at different QD/polymer ratios (by weight): (A) 0, (B) 0.09, (C) 0.18, and (D) 0.34. The samples were transferred to 2-PrOH prior to preparing the TEM grids.

micelles, as shown in Figure 3. This result is in contrast with the co-assembly of PS-*b*-P4VP with CdSe/TOPO QDs that we reported previously (29), where the co-assembly of CdSe/TOPO QDs and diblock copolymer did not affect the shape or the width of the size distribution of the spherical micelles formed and had only a very small affect on their mean diameter.

To better understand how the QD/polymer interaction affects the self-assembly of PS_{577}−$P4VP_{302}$−PEO_{852} in $CHCl_3$/2-PrOH, we examined the micellar morphologies by TEM of a series of samples prepared at different QD/polymer ratios. Figure 4 shows representative low-magnification TEM images of these samples. High-magnification images are presented in Supporting Information (Figure S4). In the absence of QDs, PS_{577}−$P4VP_{302}$−PEO_{852} formed worm-like micelles with varying lengths, accompanied by a relatively small amount of spherical micelles (Figure 4A). In addition, more complex morphologies, such as loops, buds, T-, and Y-junctions, were associated with some worm-like micelles. These morphological features make it difficult to analyze statistically the length of these worm-like micelles. Nevertheless, several micelles with lengths extended over 500 nm can be seen in Figure 4A. The overall morphology was largely maintained when a small amount of QDs (QD/polymer weight ratio 0.09) was present during self assembly (Figure 4B). In contrast, the micelle morphology changed dramatically when the weight ratio of the QD/polymer increased to 0.18 (Figure 4C). Here, most of the micelles appeared spherical, accompanied by a small number of short rods (l < 200 nm). When the weight ratio of the QD/polymer was increased to 0.34 (Figure 4D), the few remaining worm-like micelles were even shorter than those shown in Figure 4C.

In summary, as the ratio of QDs to triblock copolymer was increased, the number of worm-like composite micelles decreased, and the worm-like structures formed became shorter, accompanied by an increasing number of spherical hybrid micelles. At the highest QD/polymer ratio examined (4:1, Figure 3), we observed only spherical structures. These results clearly show that the interaction between PS_{577}−$P4VP_{302}$-PEO_{852} and CdSe(605) QDs plays an important role in the co-assembly of these two components in solution. In addition, what appear to be free QDs can be seen in the TEM images of these hybrids. Even at the lowest QD/polymer ratio (0.09), free QDs can be seen in dark-field TEM at high magnification (Figure S4, Supporting Information). As the ratio of QD/polymer was increased, both the amount of the QDs attached to the micelles and the number of free QDs increased.

There are several factors that may contribute to the conformational transition shown in Figure 4 as the QD/polymer ratio was increased. First, the selective interaction between the P4VP block of PS_{577}−$P4VP_{302}$−PEO_{852} and CdSe QDs may affect the volume of the P4VP corona, thus changing its contribution to the shape of the micelle. Second, the Flory−Huggins parameters (χ_{AB} and χ_{BC}, where A, B, C represent respectively the PS, P4VP, and PEO blocks in PS_{577}−$P4VP_{302}$−PEO_{852}) could also change due to the QD/P4VP interaction. Third, as some PS_{577}−$P4VP_{302}$−PEO_{852} molecules anchored on free QDs do not participate in the micellar self-assembly, it is possible that the increase of the QD/polymer ratio results in a decrease of the faction of polymer molecules involved in the micellar self-assembly.

3.4. Centrifugation and Redispersion of CdSe(605)/PS_{577}−$P4VP_{302}$−PEO_{852} Hybrid Micelles. In an attempt to separate the hybrid micelles formed at a QD/polymer ratio of 4:1 (by weight) from the free QDs in the sample, solutions containing both CdSe(605)/PS_{577}−$P4VP_{302}$-PEO_{852} hybrid micelles and polymer-stabilized QDs were centrifuged, separated from the supernatant fluid, and redispersed in 2-PrOH. We anticipated that the larger hybrid micelle would sedi-

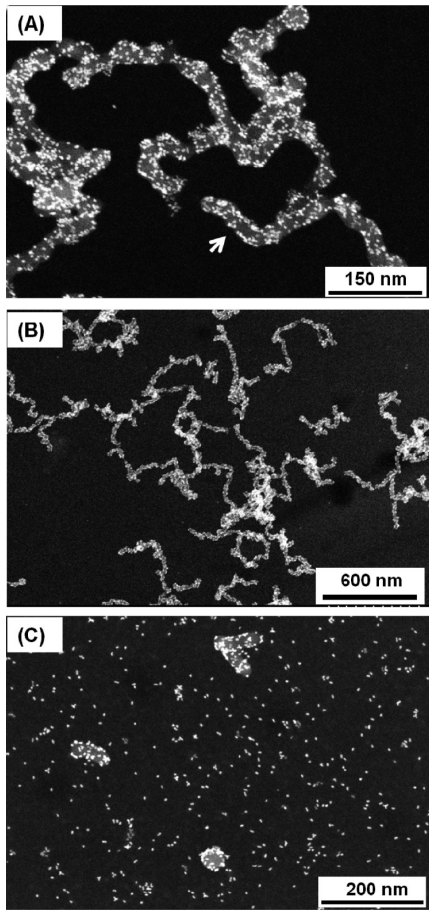

FIGURE 5. TEM (dark-field) images of the hybrid micelles of CdSe(605)/PS_{577}−$P4VP_{302}$−PEO_{852} (4:1 w/w, prepared in 3:8 v/v $CHCl_3$/2-PrOH and transferred to 2-PrOH) after centrifugation at 14 000 rpm for 30 min. (A) and (B) are images of the sediment after redispersion in 2PrOH (different magnifications). The white arrow in (A) highlights part of the continuous cylindrical structure. (C) is obtained from the supernatant following centrifugation.

ment more quickly, leaving the free QDs in suspension. For example, when a solution in 2-PrOH corresponding to the TEM image in Figure 3 was subjected to centrifugation at 14 000 rpm for 30 min, a substantial amount of colored material was pelleted at the bottom of the centrifuge tube, leaving a supernatant much less intensely colored than before. When the sediment was redispersed in 2-PrOH using mild sonication, stable colloidal solutions formed. As shown in Figure 5A, there were no free QDs in the resuspended sediment. The TEM images demonstrate the effectiveness of separating the individual quantum dots by centrifugation. A TEM image of the supernatant (Figure 5C) showed mostly free QDs plus occasional spherical hybrid micelles.

The most surprising result, however, was the nature of the hybrid structures obtained when the sediment was redispersed in 2-PrOH. There were no individual spherical hybrid micelles. Instead, we found elongated and branched structures (Figure 5A) that appeared to be formed from attachment of spherical building blocks. Some regions (for example the white arrow at the bottom center of Figure 5A) appear to have evolved into a continuous cylindrical shape. Another view of this sample at lower magnification is presented in Figure 5B. Here one gets a sense of the finite nature of the elongated structures, the importance of branching, and the overall uniformity of the sample.

These structures have many features in common with the CdSe/PS-P4VP copolymer hybrid micelles that we have examined in some detail over the past two years. While CdSe(605)/PS_{404}−$P4VP_{76}$ formed colloidally stable spherical hybrid structures when 2-PrOH was added to a solution of the polymer plus QDs in $CHCl_3$ (29), subjecting this solution to vigorous magnetic stirring led to a morphology transformation (48). Finite networks were formed. These consisted of cylindrical struts, both linear and looped, connected by Y- and T-junctions. This transformation took place only over a narrow range of solvent compositions (close to 3:8 $CHCl_3$/2-PrOH, v/v). All the results pointed to micelle fusion involving QDs bridging adjacent micelles, followed by fusion of the PS core and rearrangement to a cylindrical structure. If the $CHCl_3$ was removed prior to stirring, leaving the hybrid micelles in 2-PrOH, this morphology transformation did not occur, but some aggregation of spherical micelles was observed. For the CdSe(605)/PS_{577}−$P4VP_{302}$−PEO_{852} micelle system in 2-PrOH examined here, we speculate that spherical hybrid micelles fuse upon the sedimentation during centrifugation, and the PEG chains and the solvent-swollen P4VP blocks play a role in the subsequent morphology evolution. The QD/PS_{577}−$P4VP_{302}$−PEO_{852} triblock copolymer micelle system appears to be much less sensitive to solvent composition (i.e., the presence and amount of $CHCl_3$) than the QD/PS_{404}−$P4VP_{76}$ diblock copolymer micelle system studied previously. We can rationalize this difference in behavior in terms of the much larger fraction of the polymer composition in the triblock copolymer that is soluble in 2-PrOH than in the diblock copolymer.

3.5. Co-assembly of MEH−PPV, CdSe(605), and PS_{577}−$P4VP_{302}$−PEO_{852}. In our initial publication (29) of the co-assembly of CdSe QDs and PS_{404}−$P4VP_{76}$ diblock copolymer in $CHCl_3$/2-PrOH mixtures, we showed that three-component spherical hybrid structures could be formed with QDs in the corona of the block copolymer micelles, and poly(3-hexylthiophene) (P3HT), a conjugated polymer, confined to the PS core of the micelle. We rationalized the ability of these block copolymer micelles to solubilize P3HT in terms of the similar solubility parameters of PS and P3HT (29, 49). This same type of argument would suggest that poly(1-methoxy-4-(2-ethylhexyloxy)-p-phenylenevinylene) (MEH-PPV), another conjugated polymer, might be sufficiently compatible with PS as to be solubilized by PS_{577}−$P4VP_{302}$−PEO_{852} micelles. We first examined this idea by preparing triblock copolymer micelles in a $CHCl_3$/2-PrOH mixture by adding 4.0 mL 2-PrOH to a solution of MEH−PPV (0.1 mg) + PS_{577}−$P4VP_{302}$−PEO_{852} block copolymer (2.0 mg) in chloroform (1.5 mL). In this way, we obtained a transparent highly colored (pink) and fluorescent solution with an absorbance maximum at 514 nm. As shown in Figure 6A, these micelle have a robust colloidal stability and do not sediment appreciably when centrifuged 90 min at 14 000 rpm.

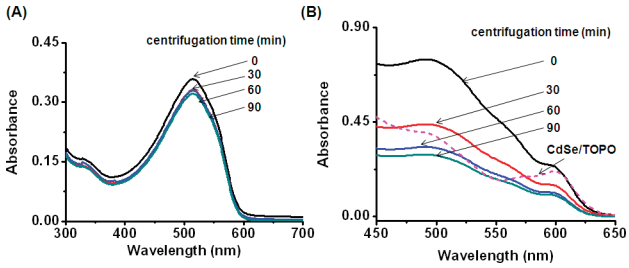

FIGURE 6. (A) UV−vis absorption spectra of the composite micelles formed by PS_{577}−$P4VP_{302}$−PEO_{852} and MEH−PPV in 2-PrOH before centrifugation and the supernatant after different periods of centrifugation (14 000 rpm). (B) UV−vis absorption spectra of the hybrid micelles formed by PS_{577}−$P4VP_{302}$−PEO_{852}, MEH−PPV, and CdSe(605)/TOPO in 2-PrOH before centrifugation and the supernatant after different periods of centrifugation (14 000 rpm). The final solution contained 0.25 mg/mL PS_{577}−$P4VP_{302}$−PEO_{852} and 0.34 mg/mL QDs. The dashed curve shows the absorption spectrum of CdSe(605)/TOPO in toluene.

This ternary hybrid system was prepared by dissolving 2.7 mg of CdSe(605) QDs, 2.0 mg of triblock copolymer, and 0.10 mg of MEH-PPV (M_w = 80 000) in $CHCl_3$, adding 2-PrOH to a solvent ratio of 3:8 (v/v), and then stirring 10 min. At this point, the $CHCl_3$ was stripped off on a rotary evaporator, and the solution was diluted to 8 mL of 2-PrOH. A UV−vis spectrum of this solution in 2-PrOH is presented in the uppermost curve of Figure 6B. By comparing this spectrum to that of the QDs in toluene (dashed curve in Figure 6B) and the MEH−PPV spectrum in Figure 6A, we see that the spectrum of the ternary hybrid shows additive absorption from both CdSe(605) QD and MEH−PPV.

We tested this solution by centrifugation to see if we could obtain more quantitative information about which species remained in solution following sedimentation of the larger hybrids. The spectra in Figure 6B show that after centrifugation at 14 000 rpm for 30, 60, and 90 min that there is still significant absorption at the maximum of the MEH−PPV component, as well as the band edge absorption of the QDs at 605 nm. By assuming additive absorption of these two components, we calculate that 38% of the QDs and about 40% of the MEH−PPV were separated into the sediment after 30-min centrifugation, that is, simultaneous sedimentation of both CdSe(605) QDs and MEH−PPV. A TEM image taken from a solution obtained by redispersion of the sediment in 2-PrOH showed elongated network-like structures and no free micelles (Figure S5, Supporting Information). Additional centrifugation (60 min, 90 min) led to additional sedimentation. Analysis of the UV−vis spectrum in Figure 6B for 90 min centrifugation suggests that 60% of the QDs and 70% of the MEH−PPV sedimented under these conditions.

3.6. Co-assembly of PS_{577}−$P4VP_{302}$−PEO_{852}, MEH−PPV, and CdSe/ZnS Core/Shell QDs. To explore the generality of the hybrid self-assembly described above, we investigated the co-assembly with a different QD sample, CdSe/ZnS(485)/TOPO core/shell QDs ($d = 3 \pm 1$ nm, by TEM), which exhibit a band-edge absorption at 485 nm. As with the samples described above, the QDs (4.0 mg), triblock copolymer (1.0 mg), and MEH−PPV (0.1 mg) were dissolved in $CHCl_3$. 2-PrOH was added, and then after stirring briefly, the $CHCl_3$ was removed and replaced with 2-PrOH. As shown in Figure 7A, this procedure leads to a mixture of spherical micelles and branched worm-like structures to which many QDs are attached, accompanied by a significant number of free QDs that have acquired colloidal stability in 2-PrOH. When this solution in 2-PrOH was centrifuged, we could see by eye that it was more difficult to sediment the larger structures seen by TEM. For example, after 1 h at 14 000 rpm, some of the material pelleted at the bottom of the centrifuge tube. By visual inspection, however, we could tell that most of the material remained in the supernatant. The TEM image (Figure 7D) from the supernatant also shows a significant amount of spherical hybrid micelles coexisting with many free QDs. These results imply that it was more difficult to separate the hybrid micelles of PS_{577}−$P4VP_{302}$−PEO_{852}/[CdSe/ZnS(485)]/MEH−PPV than hybrid micelles of PS_{577}−$P4VP_{302}$−PEO_{852}/CdSe(605)/MEH-PPV. This difference may be connected to the smaller size of the CdSe/ZnS(485) core/shell QDs, which would make the density of the hybrid micelles less than that of the corresponding CdSe(605) structures. Nevertheless, we imagine that better separation would be possible under a higher centrifugation speed.Figures 7B−C show dark-field TEM images of the sediment of PS_{577}−$P4VP_{302}$−PEO_{852}/[CdSe/ZnS(485)]/MEH-PPV micelles, following redispersion in 2-PrOH. Again, one can discern branched cylindrical micelles with QD particles attached to the surface. In addition, a very small number of free QD particles were observed by dark-field TEM in the samples prepared from the redispersed sediment. We speculate that these free QD particles were part of the network structures when they were sedimented but dissociated upon redispersion. It is possible that there is weaker adhesion of the smaller CdSe/ZnS(485) core/shell particles to the P4VP coronae of the micelles that of the CdSe(605) QDs.

4. SUMMARY

In solvent mixtures of $CHCl_3$ and 2-PrOH, the triblock copolymer, PS_{577}−$P4VP_{302}$−PEO_{852} self-assembled into worm-like micelles with a diameter of ~25 nm accompanied by a small population of spherical micelles with $d = 34$ nm. When 2-PrOH was added to a mixed solution of TOPO-coated CdSe(605) nanocrystals (QDs) and the triblock copolymer in $CHCl_3$, co-assembly took place to form hybrid micelles in which the morphology depended on the QD/polymer ratio. The $CHCl_3$ was then selectively distilled off, and the samples were diluted to known concentrations in 2-PrOH. The overall length of the worm-like micelles decreased gradually as the ratio of QD/polymer was increased and finally evolved exclusively into spherical micelles when the QD/polymer ratio reached 4:1 by weight. Within these structures, the QDs could be seen in dark-field TEM images to decorate the outer edge of the insoluble PS core. We presume that the pyridine groups of the P4VP component of the block copolymer displaced TOPO groups from the QD surface and became bound to the QDs as a multidentate ligand (15, 17, 22, 32). Thus the QDs became incorporated into the P4VP domains of the micelles.

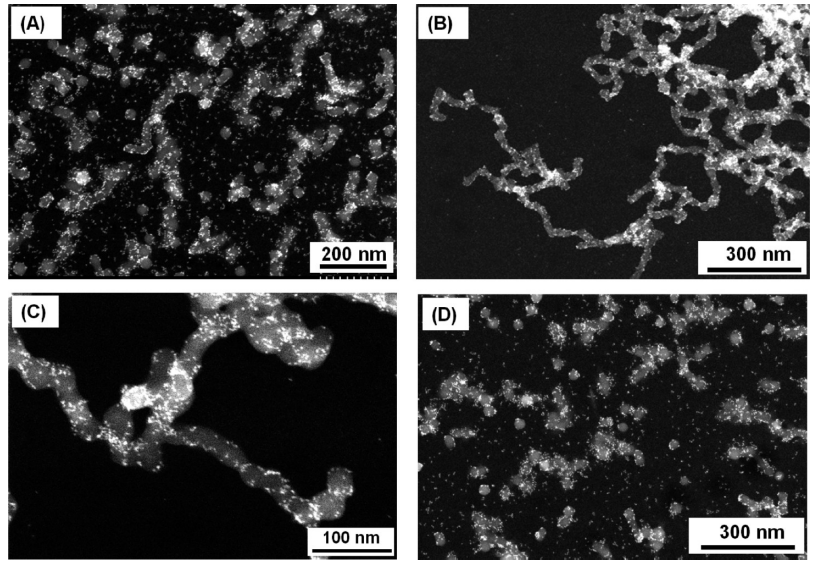

FIGURE 7. TEM (dark-field) images of the ternary hybrid micelles formed by PS_{577}−$P4VP_{302}$−PEO_{852}, MEH-PPV, and CdSe/ZnS(485)/TOPO core/shell QDs: (A) as-prepared micelles from 3:8 (v/v) $CHCl_3$/2-PrOH; (B, C) images at different magnifications from the sediment obtained by centrifugation (14,000 rpm, 1 h), followed by redispersion in 2-PrOH; (D) the supernatant after centrifugation.

These structures exhibited much greater colloidal stability in 2-PrOH and in $CHCl_3$/2-PrOH mixtures than a system studied previously consisting of PS_{404}-$P4VP_{76}$ diblock copolymer and very similar CdSe QDs. For example, the triblock copolymer formed stable micelles at much higher QD/polymer weight ratios than was possible for the diblock copolymer, and morphological changes occurred for the hybrid triblock copolymer assemblies for alcohol-rich media in which the hybrid diblock copolymer assemblies were kinetically frozen. One of the major differences between the two systems is that the diblock copolymer has a long PS block and a much shorter P4VP block, leading to the formation of crew-cut micelles with a rather thin P4VP corona. Overloading of the corona with QDs leads to bridging interactions that can cross-link the micelles. The PS_{577}−$P4VP_{302}$−PEO_{852} triblock copolymer has a somewhat longer PS block, but a substantially longer P4VP block, as well as a long PEO block. With the QDs confined to the P4VP domains, the PEO chains provide a robust steric barrier to promote colloidal stability.

Accompanying formation of the QD/triblock copolymer hybrid micelles were individual QDs that became soluble (or dispersible) in 2-PrOH. Since CdSe/TOPO is insoluble in 2-PrOH, we imagine that one or more block copolymer molecules became attached to the QDs through displacement of TOPO groups with pyridine units from the polymer. We were able to sediment selectively the larger spherical micelles formed at a QD/polymer weight ratio of 4:1 from the individual QDs that remained in colloidal solution. Within the sediment, and with subsequent redispersion in 2-PrOH, a remarkable morphology transformation occurred. The redispersed structures were very long, branched cylindrical objects coated with QDs.

When micelles were formed from the triblock copolymer in the presence of small amounts of the conjugated polymer MEH−PPV, the MEH−PPV was solubilized by the micelles giving intensely colored solutions whose UV−Vis spectra were the sum of the contributions of the QDs and conjugated polymer. Three-component hybrid micelles were formed under similar conditions, with the overall micelle morphology unaffected by the amounts of MEH-PPV used in the sample preparation. Because MEH-PPV and polystyrene have similar solubility parameters, we believe that the conjugated polymer in these structures is confined to the PS core of the micelles. Similar structures were formed when we employed smaller ($d = 3.1$ nm) CdSe/ZnS(485) core-shell QDs, with a band edge absorption at 405 nm instead of the larger CdSe(605) QDs ($d = 5.1$ nm). These hybrid micelles were more resistant to sedimentation than those formed from the larger QDs. The smaller fraction that sedimented could be redispersed in 2-PrOH, and formed similar (by TEM) branched cylindrical and network structures to those observed upon redispersion of the sedimented hybrids formed with the larger QDs.

These experiments demonstrate some of the fascinating QD-micelle hybrid structures that one can create by self assembly with combinations of block copolymer, QDs, and conjugated polymer. Particularly interesting in the results presented here are the examples in which the presence and amount of QDs in the mixture affect and control the morphology of the self assembled structures obtained.

Acknowledgment. We are grateful to Dr. Margret Hines at Evident Technology for providing the CdSe/ZnS core/shell QDs. We thank NSERC Canada for support of this research.

Supporting Information Available: TEM images of PS_{577}−$P4VP_{302}$−PEO_{852} micelles after being diluted in 2-PrOH and a treatment in a sonicator bath; AFM images of PS_{577}−$P4VP_{302}$−PEO_{852}/CdSe(605) micelles; TEM images of PS_{577}−$P4VP_{302}$−PEO_{852}/CdSe(605) micelles formed from the QD/polymer mixture with and without multiple precipitation in *n*-hexane and redispersion in $CHCl_3$; high-resolution TEM images of PS_{577}−$P4VP_{302}$−PEO_{852}/CdSe(605) micelles with different polymer/QD ratios; a TEM (dark-field) image of the

hybrid micelles formed by PS_{577}−$P4VP_{302}$−PEO_{852}, MEH−PPV, and CdSe(605)/TOPO QDs from the sediment of centrifugation (14 000 rpm, 0.5 h), followed by redispersion in 2-PrOH. This information is available free of charge via the Internet at http://pubs.acs.org.

REFERENCES AND NOTES

(1) Bockstaller, M. R.; Michiewicz, R. A.; Thomas, E. L. *Adv. Mater.* **2005**, *17*, 1331.
(2) Balazs, A. C.; Emrick, T.; Russell, T. P. *Science* **2006**, *314*, 1107.
(3) Rozenberg, B. A.; Tenne, R. *Prog. Polym. Sci.* **2008**, *33*, 40.
(4) Tomczak, N.; Janczewski, D.; Han, M. Y.; Vancso, G. J. *Prog. Polym. Sci.* **2009**, *34*, 393.
(5) Greenham, N. C.; Peng, X. G.; Alivisatos, A. P. *Phys. Rev. B* **1996**, *54*, 17628.
(6) Wang, M.; Kumar, S.; Coombs, N.; Scholes, G. D.; Winnik, M. A. *Macromol. Chem. Phys.* **2009**, *211*, 393.
(7) Colvin, V. L.; Schlamp, M. C.; Alivisatos, A. P. *Nature* **1994**, *370*, 354.
(8) Huynh, W. U.; Dittmer, J. J.; Alivisatos, A. P. *Science* **2002**, *295*, 2425.
(9) Murray, C. B.; Norris, D. J.; Bawendi, M. G. *J. Am. Chem. Soc.* **1993**, *115*, 8706.
(10) Jun, Y. W.; Choi, J. S.; Cheon, J. *Angew. Chem. Int. Ed.* **2006**, *45*, 3414.
(11) Park, J.; Joo, J.; Kwon, S. G.; Jang, Y.; Hyeon, T. *Angew. Chem., Int. Ed.* **2007**, *46*, 4630.
(12) Wang, Y. A.; Li, J. J.; Chen, H. Y.; Peng, X. G. *J. Am. Chem. Soc.* **2002**, *124*, 2293.
(13) Guo, W. H.; Li, J. J.; Wang, Y. A.; Peng, X. G. *J. Am. Chem. Soc.* **2003**, *125*, 3901.
(14) Kim, S.; Bawendi, M. G. *J. Am. Chem. Soc.* **2003**, *125*, 14652.
(15) Skaff, H.; Emrick, T. *Chem. Commun.* **2003**, 52.
(16) Liu, J. S.; Tanaka, T.; Sivula, K.; Alivisatos, A. P.; Frechet, J. M. J. *J. Am. Chem. Soc.* **2004**, *126*, 6550.
(17) Wang, X.-S.; Dykstra, T. E.; Salvador, M. R.; Manners, I.; Scholes, G. D.; Winnik, M. A. *J. Am. Chem. Soc.* **2004**, *126*, 7784.
(18) Kim, S. W.; Kim, S.; Tracy, J. B.; Jasanoff, A.; Bawendi, M. G. *J. Am. Chem. Soc.* **2005**, *127*, 4556.
(19) Nann, T. *Chem. Commun.* **2005**, 1735.
(20) Potapova, I.; Mruk, R.; Hubner, C.; Zentel, R.; Basche, T.; Mews, A. *Angew. Chem., Int. Ed.* **2005**, *44*, 2437.
(21) Uyeda, H. T.; Medintz, I. L.; Jaiswal, J. K.; Simon, S. M.; Mattoussi, H. *J. Am. Chem. Soc.* **2005**, *127*, 3870.
(22) Wang, M.; Oh, J. K.; Dykstra, T. E.; Lou, X.; Scholes, G. D.; Winnik, M. A. *Macromolecules* **2006**, *39*, 3664.
(23) Wang, M.; Dykstra, T. E.; Lou, X. D.; Salvador, M. R.; Scholes, G. D.; Winnik, M. A. *Angew. Chem., Int. Ed.* **2006**, *45*, 2221.
(24) Zubarev, E. R.; Xu, J.; Sayyad, A.; Gibson, J. D. *J. Am. Chem. Soc.* **2006**, *128*, 4958.
(25) Wang, M.; Felorzabihi, N.; Guerin, G.; Haley, J. C.; Scholes, G. D.; Winnik, M. A. *Macromolecules* **2007**, *40*, 6377.
(26) Zhang, T. R.; Ge, J. P.; Hu, Y. P.; Yin, Y. D. *Nano Lett.* **2007**, *7*, 3203.
(27) Duan, H. W.; Nie, S. M. *J. Am. Chem. Soc.* **2007**, *129*, 3333.
(28) Xu, J.; Wang, J.; Mitchell, M.; Mukherjee, P.; Jeffries-El, M.; Petrich, J. W.; Lin, Z. Q. *J. Am. Chem. Soc.* **2007**, *129*, 12828.
(29) Wang, M.; Kumar, S.; Lee, A.; Felorzabihi, N.; Shen, L.; Zhao, F.; Froimowicz, P.; Scholes, G. D.; Winnik, M. A. *J. Am. Chem. Soc.* **2008**, *130*, 9481.
(30) Lin, W.; Fritz, K.; Guerin, G.; Bardajee, G. R.; Hinds, S.; Sukhovatkin, V.; Sargent, E. H.; Scholes, G. D.; Winnik, M. A. *Langmuir* **2008**, *24*, 8215.
(31) Shen, L.; Pich, A.; Fava, D.; Wang, M. F.; Kumar, S.; Wu, C.; Scholes, G. D.; Winnik, M. A. *J. Mater. Chem.* **2008**, *18*, 763.
(32) Shen, L.; Soong, R.; Wang, M. F.; Lee, A.; Wu, C.; Scholes, G. D.; Macdonald, P. M.; Winnik, M. A. *J. Phys. Chem. B* **2008**, *112*, 1626.
(33) Wang, M.; Zhang, M.; Qian, J. S.; Zhao, F.; Shen, L.; Scholes, G. D.; Winnik, M. A. *Langmuir* **2009**, *25*, 11732.
(34) Wang, M.; Zhang, M.; Siegers, C.; Scholes, G. D.; Winnik, M. A. *Langmuir* **2009**, *25*, 13703.
(35) Wang, M.; Bardajee, G. R.; Kumar, S.; Nitz, M.; Scholes, G. D.; Winnik, M. A. *J. Chromatogr. A* **2009**, *1216*, 5011.
(36) Skaff, H.; Emrick, T. *Angew. Chem., Int. Ed.* **2004**, *43*, 5383.
(37) Skaff, H.; Sill, K.; Emrick, T. *J. Am. Chem. Soc.* **2004**, *126*, 11322.
(38) Moffitt, M.; Eisenberg, A. *Chem. Mater.* **1995**, *7*, 1178.
(39) Moffitt, M.; McMahon, L.; Pessel, V.; Eisenberg, A. *Chem. Mater.* **1995**, *7*, 1185.
(40) Wang, J. Y.; Chen, W.; Liu, A. H.; Lu, G.; Zhang, G.; Zhang, J. H.; Yang, B. *J. Am. Chem. Soc.* **2002**, *124*, 13358.
(41) Zhang, M. F.; Drechsler, M.; Muller, A. H. E. *Chem. Mater.* **2004**, *16*, 537.
(42) Yan, X. H.; Liu, G. J.; Haeussler, M.; Tang, B. Z. *Chem. Mater.* **2005**, *17*, 6053.
(43) Wang, X. S.; Wang, H.; Coombs, N.; Winnik, M. A.; Manners, I. *J. Am. Chem. Soc.* **2005**, *127*, 8924.
(44) Tamborra, M.; Striccoli, M.; Curri, M. L.; Alducin, J. A.; Mecerreyes, D.; Pomposo, J. A.; Kehagias, N.; Reboud, V.; Torres, C. M. S.; Agostiano, A. *Small* **2007**, *3*, 822.
(45) Zhang, L. F.; Eisenberg, A. *Science* **1995**, *268*, 1728.
(46) Gohy, J. F. *Adv. Polym. Sci.* **2005**, *190*, 65.
(47) Zhang, L. F.; Eisenberg, A. *Macromolecules* **1999**, *32*, 2239.
(48) Zhang, M.; Wang, M. F.; He, S.; Qian, J. S.; Saffari, A.; Lee, A.; Kumar, S.; Hassan, Y.; Guenther, A.; Scholes, G.; Winnik, M. A. *Macromolecules* **2010**, *43*, 5066.
(49) Li, W.; Maddux, T.; Yu, L. *Macromolecules* **1996**, *29*, 7329.

AM100645J